Article ID: 1007-1202(1999)04-0439-06

Ionospheric Responses to a Total Solar Eclipse Deduced by the GPS Beacon Observations*

CHEN An-hua, YU Sheng-bing, XU Ji-sheng
College of Electronic Information, Wuhan University, Wuhan 430072, China

Abstract: The total electron content (TEC) data during the total eclipse of March 9, 1997 were collected, which were observed by means of nine GPS receivers located at the eastern Asia. The responses of total TEC to the eclipse were analyzed. The results show that: 1) the eclipse led to apparent decrement in TEC that lasted for six to eight hours; 2) the maximum decrement occurred after the middle of the eclipse with time-delays varying from twenty minutes to about three hours; 3) the maximum absolute deviations of TEC on the eclipse day do not show a simple and consistent relationship to the maximum solar obscuration.

Key words: solar eclipse; ionosphere; total electron content; GPS beacon
CLC number: P 352.2 **Document code**: A

0 Introduction

Observations about the solar eclipses and the lunar eclipses have been recorded for more than 2 500 years while their effects on the ionosphere were noticed only seventy years ago. In the early stage, ionosonde was a main tool for monitoring ionospheric responses to solar eclipses. Since the 1960's, however, beacon satellites have been applied to investigate ionospheric behavior during eclipses. With the developing of monitoring tools and technique, a serious of fruitful results about ionospheric photochemistry and the dynamic processes during eclipses have been obtained[1-6].

A new era of making TEC measurements has begun with the use of dual-frequency beacons transmitted by the Global Positioning System (GPS). The global coverage, convenient receiver sources and other attractive advantages ensure its extensive application. Recently, the total electron content data observed by means of nine GPS receivers located at the eastern Asia were collected during the total eclipse of March 9, 1997. A comprehensive analysis on responses of total electron content (TEC) to this eclipse was made. In this paper the data processing method is first described; then, some results and a brief discussion about eclipse-caused dynamic effects on the ionosphere are presented.

1 Data and their processing method

1.1 Form of TEC data

Producing ionospheric TEC data obtained by the dual-frequency GPS receivers requires a conversion of the raw GPS range data to the TEC along the line of sight, i. e. the slant TEC. Two types of delay observables are available from each station-to-satellite line of sight measurement, namely, the group delay and carrier-phase. Each observable was acquired at frequencies of f_1 (1.227 6 GHz) and f_2 (1.575 42 GHz) with a 30 s time interval.

The integration of electron content along the line of sight can be deduced by two ways. According to the theory of radio wave propagation in the ionosphere, the differential group delay and the differential carrier phase at the two frequencies both are proportional to the slant TEC. Let TEC_S^g and TEC_S^φ represent the slant TEC deduced from

Received date: 1999-06-15
* Foundation item: Supported by the National Natural Science Foundation of China(49684002)
Biography: CHEN An-hua(1976-), female, Master candidate. Research interests: studying ionosphere by GPS beacons.

the differential group delay ($P_2 - P_1$) and the differential carrier phase ($\Phi_1 - \Phi_2$), respectively. Then, for a given time and a fixed receiver, they are given as follows,

$$TEC^{a;i}_{s;jk} = 9.518 \times (P^i_{2j,k} - P^i_{1j,k} - \Delta d) \quad (1)$$

$$TEC^{r;i}_{s;jk} = 9.518 \times (\lambda_1 \phi^i_{1j,k} - \lambda_2 \phi^i_{2j,k} - A^i_j - \Delta b) \quad (2)$$

where i, j denote the order of satellites and receivers, k is the order of data points, λ_1 and λ_2 are wave lengths of two carriers, A^i_j is the unknown phase integral constant, Δd and Δb denote the biases due to instrumental biases, multipath effects and cycle slips. Cycle-slips are detected by comparing consecutive value of TEC^r_S and arc connection is done by fitting a polynomial to the epochs before or after the cycle-slip.

Receiver and satellite clock errors in the pseudorange were removed in the differencing. However, instrumental biases in both the receiver and GPS satellite transmitters still remained. Besides, it is hard to remove the error due to multipath effects. It is well known, in fact, that they significantly affect the value of The slant TEC. The differential carrier phase ($L_1 - L_2$) is negative and, although inherently more precise than the pseudorange, is biased by an integer cycle ambiguity. The slant TEC was formed by combining use of the pseudorange and carrier phase data in accordance to the following procedure. All the phase data were adjusted by a constant to match the absolute level of the pseudorange. The constant was then computed so as to minimize the root-mean-square difference between pseudorange and phase differential delay calculated over the arc, such that :

$$A^{rs} = \frac{1}{N}\sum_{i=1}^{N}\{(P^{rs}_{1i} - P^{rs}_{2i}) - (L^{rs}_{2i} - L^{rs}_{1i})\} \quad (3)$$

where N is the number of measurements in a phase-connected arc of data for a given receiver r and satellite s. For each datum i, the pseudorange delays are denoted by P^{rs}_{1i} and P^{rs}_{2i} for the f_1 and f_2 frequencies, respectively; the corresponding phase delays are L^{rs}_{1i} and L^{rs}_{2i}. The slant TEC for measurement i becomes:

$$TEC_i = K[A^{rs} + (L^{rs}_{2i} - L^{rs}_{1i})] \quad (4)$$

where $K = 2.85$. The left side of Eq. (4) is the slant TEC expressed in the TEC unit of $10^{16}/m^2$.

In order to compare electron contents for paths with different elevation angles, The slant TEC must be converted into equivalent vertical TEC. The slant TEC is related to an equivalent vertical TEC by:

$$TEC^v_i = TEC_i \cos \chi \quad (5)$$

Where χ is the zenith angle of the line of sight at the sub-ionospheric point and can be deduced by:

$$\chi = \arcsin\left[\frac{r_e}{r_e + h} \times \cos \alpha\right] \quad (6)$$

Where α is the elevation of the satellite, r_e is the mean radius of the earth and h is the height of sub-ionospheric point, which was taken as 400 km in this paper.

1.2 Eclipse condition and observations

On March 9, 1997, a total solar eclipse took place. Its path of totality started in Northern Asia and ended in Arctic Ocean, skirting Mongolia, East-northern China and Russia. Total eclipse or partial eclipse can be observed in most part of Asia.

We have collected GPS data of nine stations. The latitude and longitude of them range in 25°-53° N and 91°-114° E respectively. The maximum obscuration of the sun varies from 45% to 100% in this region. Table 1 lists the coordinates (which were obtained by GPS positioning technique) and eclipse condition for each receiving station.

1.3 A note of processing method

To extract the eclipse effects, the average value of the diurnal TEC on both pre-eclipse day and post-eclipse day was taken as the reference level, and the deviations of the diurnal TEC on the eclipse day from the reference level were then calculated.

There are several questions needed to be concerned about when such a procedure was made. The first question is that the GPS is the orbiting satellites system so both TEC temporal and special variations need to be concerned when comparing TEC on the eclipse day with reference level. The orbit for the same satellite changes little on these adjacent three days because the rotation period of the GPS satellites is about 12 h. Therefore it is reasonable to use TEC deviations during the eclipse from a reference level obtained on the basis of TEC measurements one day before and one day after the eclipse to measure the effect of the eclipse on the

Table 1 Coordinates and eclipse condition of the receiving stations

Station	Geographic latitude	Geographic longitude	First contact /BST	Middle of Eclipse/BST	Last contact /BST	Local time	Percent obscuration/%
Shao	31°06′	121°12′	7:29	8:32	9:42	UT+8	60
Usud	36°08′	138°22′	7:53	9:04	10:19	UT+9	59
Taiw	25°01′	121°32′	7:24	8:23	9:28	UT+8	43
Tskb	36°06′	140°05′	7:54	9:05	10:20	UT+9	55
Irkt	52°13′	104°19′	7:54	8:54	9:59	UT+7	99
Lhas	29°40′	91°06′	-	8:14	9:09	UT+8	60
Wuhn	30°32′	114°28′	7:25	8:25	9:31	UT+8	61
Taej	36°20′	127°26′	7:40	8:47	10:01	UT+8	68
Mohe	52°58′	122°32′	8:03	9:09	10:20	UT+8	100

ionosphere.

Above procedure may give rise to the second question. It is well known, there are the so-called QBO phenomena in the ionosphere[7]. The referenced level obtained on even days can be biased in applying it as the mean value of odd days. So taking the average on more days as the reference level is a better solution as long as change of orbits for the same satellite can be neglected.

There are always the day-to-day variations of TEC in the ionosphere which are confused in the ionospheric responses to the eclipse extracted. To divide the ionospheric responses to the eclipse from the day-to-day variations of TEC, a standard deviation was calculated for all collected data except that of the eclipse day and that part exceeding the standard deviation was regarded as ionospheric effects of the eclipse.

The instrumental biases in satellite transmitters and receivers are the main source of error in the estimation of TEC and are hard to be removed. The TEC value after midnight can be distorted to below zero in some stations because of these biases. However, the temporal variation of the biases is very slow so that the variation of the biases in adjacent few days can be neglected[8]. To reduce effects of these biases, TEC absolute deviations of eclipse time from the referenced level were regarded as the index of eclipse effects in stead of absolute TEC value or the percent deviation.

2 Results

Throughout the observing days, many satellites are tracked. With depicting the TEC value of March 9, 1997 and that of the control days, the TEC depletion during eclipse hours is very obvious. To extract the eclipse effects, the deviation of the diurnal TEC from the referenced TEC value using the method mentioned above is more noticeable. Fig. 1 shows an example of such deviations of TEC observed by satellite 25 at eight stations. The traces of the sub-ionospheric points of satellite 25 during the corresponding hours on March 9, 1997 at each station are also illustrated in Fig. 2.

It can be seen from the Fig. 1 that the eclipse leads to obvious TEC depression in large scale of sub-ionospheric points. This kind of depression occurred on the neck of the first contact of the eclipse. Then the negative deviation became deeper with the area of optical disk obscured getting larger. But in most of the stations the occurrence time of maximum decrement didn't agree with the time of the middle of eclipse. The trend of depression continues after the middle of eclipse. It can be seen from the stations with data long enough to show the TEC recovery phase that the time for restoration was also delayed compared with the time of the last contact.

Because the satellites are moving all the time, so the TEC depends on both the spatial and temporal factors. It will be easy for us to compare quantitatively if one of the factors is restricted. In common cases a GPS receiver can record the group delay and carrier-phase of the dual-frequency beacons from 4-8 satellites simultaneously and the sub-ionospheric points distribute around the receiver. If the data are confined to select from a small longitudinal and latitudinal sector surrounding the receiver, the TEC's dependence on sub-ionospheric location can be suppressed. Thus we can get the TEC variation at a fixed point that is related only to the time of a day. Fig. 3 shows the deviations of TEC from referenced level as a function of time using the method mentioned above. The geographic coordinate of the station and the maximum percent obscuration are also marked in the up-right corner of each panel in the picture.

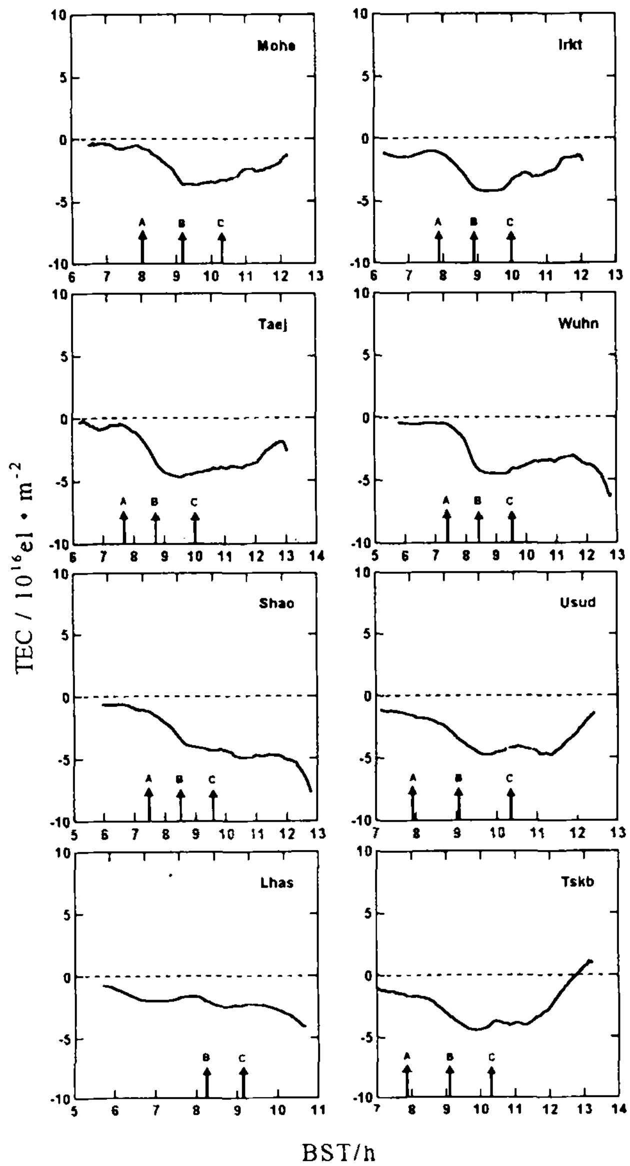

Fig. 1 Observed deviation of diurnal TEC at eight stations on the eclipse day. The arrows above the x-axis indicate the time of the first contact A, maximum eclipse B, and the last contact C

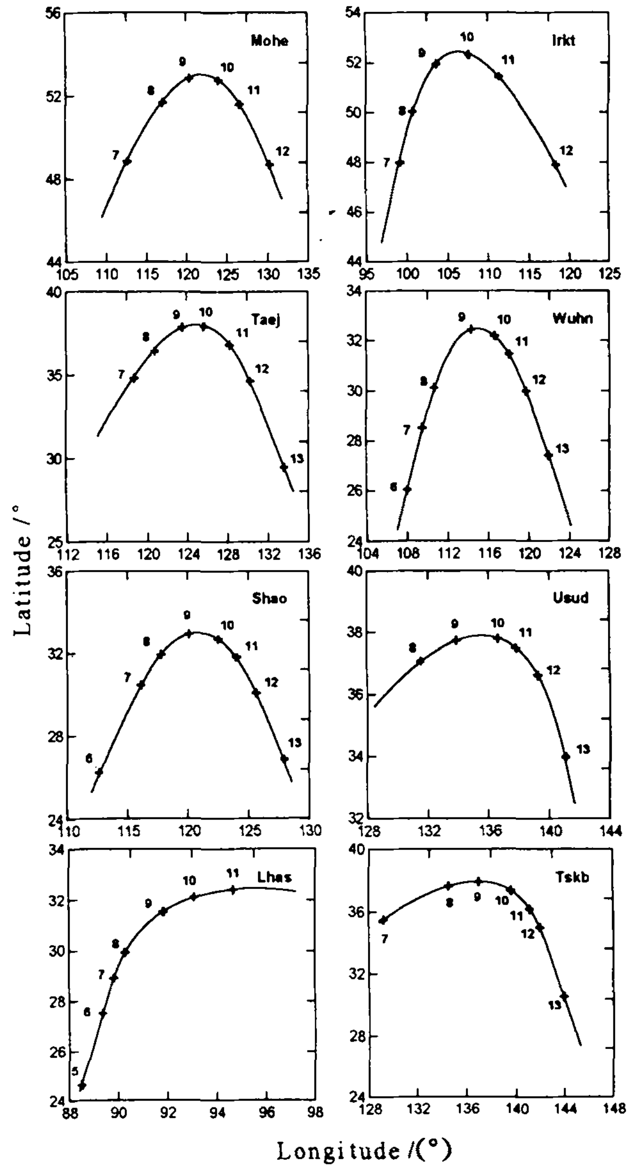

Fig. 2 The traces of the sub-ionospheric points of satellites on March 9, 1997 for each station. The numbers on the curves indicate the time (BST) when the line of sight of satellite passed by

In an attempt to reveal the underlying physical factors that play a dominant role in causing the ionospheric behavior on eclipse day, the value of the maximum deviation and the time delay of maximum decrement and TEC restoration for each station are listed in Table 2. A careful examination of Fig. 3 and Table 2 reveals three features that are coherent over at least half of the stations.

1) The eclipse led to apparent decrement in TEC that lasted for six to eight hours. An interesting phenomenon is that the TEC started to drop before the first contact of the eclipse in stations with higher latitude; such as Mohe, Irkt and Taej. This may be due to both the earlier obscuration of the corona before the obscuration of the optical disk and the time of the first contact of the eclipse at ionospheric heights is earlier than on the ground.

2) The maximum decrement occurred after the middle of the eclipse with time-delays varying from twenty minutes to about three hours. Comparing with the last contact of the eclipse, there was also

a time-delay for TEC restoring to reference level and the time-delays were different at different stations. The nearer is the location to the totality path, the smaller is the time-delay for both the maximum depletion and the restoration to the reference level.

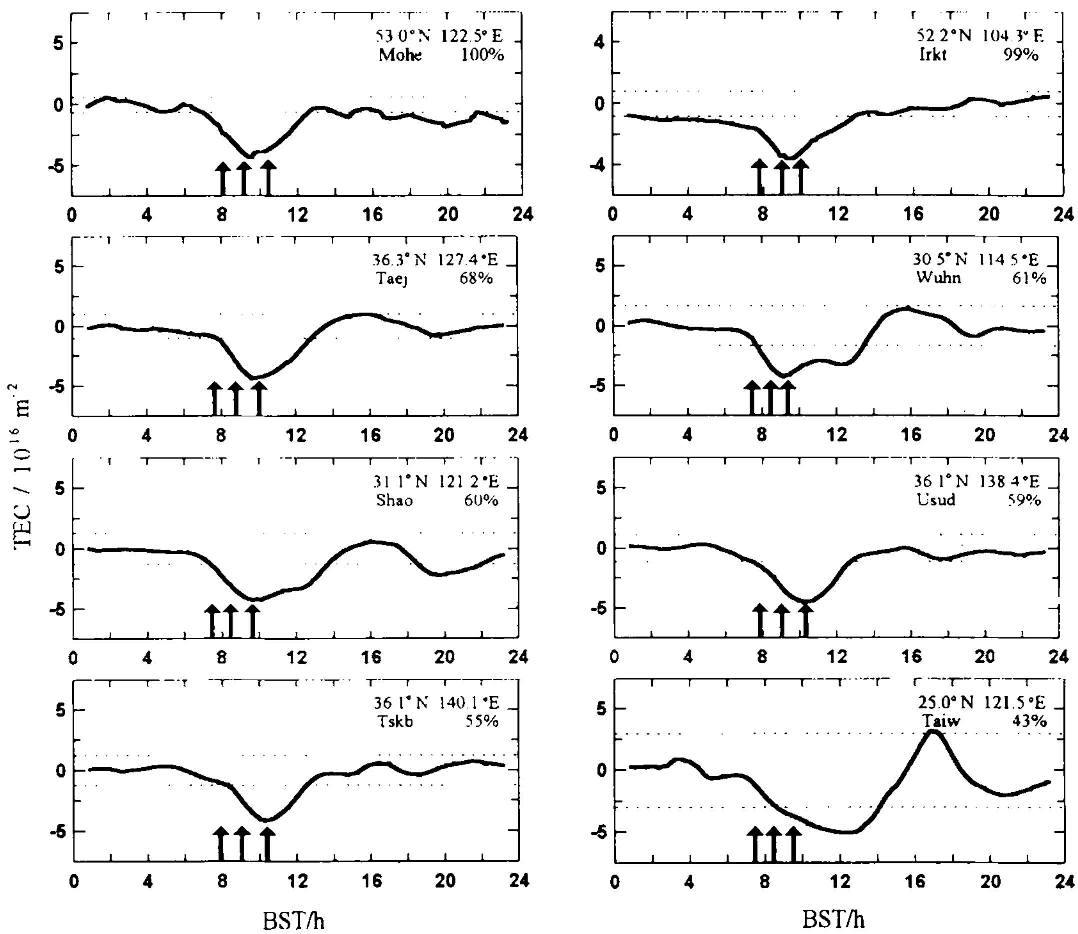

Fig. 3 TEC deviation from referenced level as a function of time. The geographic coordinate and the maximum percent obscuration at the local station are marked in the up-right corner. The dotted lines represent the standard deviation of the day-to-day variations of TEC

Table 2 The maximum TEC deviation and the time delay of the maximum decrement and the TEC restoration

Station	Maximum TEC deviation $/10^{16}m^{-2}$	Delay of TEC maximum decrement	Delay of TEC restoration	Percent obscuration/%
Mohe	−4.366 3	00:20:00	02:15:30	100
Irkt	−3.608 1	00:30:30	03:51:00	99
Taej	−4.366 4	00:51:00	03:33:00	68
Wuhn	−4.285 8	00:43:00	04:40:30	61
Shao	−4.273 1	01:06:30	05:07:30	60
Usud	−4.544 9	01:10:00	05:07:00	59
Tskb	−4.160 4	01:09:00	03:26:00	55
Taiw	−5.067 8	03:08:00	06:01:30	43

3) The maximum absolute TEC deviations on the eclipse day do not seem to show a simple and consistent relationship to the maximum solar obscuration. On the contrary, it appears that the station with the lowest geographical latitude, for example, the station Taiw, got the largest maximum TEC deviation which reached $-5.0678\times10^{16}/m^2$. It implied the transportation process in the equatorial anomaly region played an important role in ionospheric responses to the eclipse besides photo-

chemical process.

3 Discussion

A solar eclipse is a rare natural event and its effect on the ionosphere is complicated by the involving many kind of processes, including ionization, chemical reactions, ambipolar diffusion, buoyancy forces, electrodynamic drift, neutral wind effects, etc, not to mention processes coupled into the ionosphere from the magnetosphere, the thermosphere and the lower atmosphere. This explained why the inconsistent experimental results were reported in the previous publications sometimes and the difficulty in simulating the processes in the ionosphere during eclipses.

It is generally regarded that the electron density in the D, E and F_1 regions is dominated by a balance between photo-ionization and chemical recombination. Thus the hiding of the optical rays causes direct reduction in photo-ionization, destroys the previous photochemical equilibrium and results in the depletion in electron density. The transport term in the continuity equation for the ionization is very significant in the ionospheric F_2 region and it is sensitive to the electron temperature and ion temperature. The obscuration of optical disk leads to considerable decrease in the temperatures of electrons and ions but the electron temperature drops more greatly[9]. The reduced ratio of electron temperature to ion temperature may cause the downward diffusion of electrons from the topside ionosphere and leave a deficient electron density in the F_2 region[5]. This mechanism can be substantiated by the long time delay of TEC both in dropping to maximum deviation and in restoring to the normal level because the transportation process is slower to react than the photoionization process. Since total electron content is the integration of electron density along the propagation path, it is difficult to isolate contribute of various regions of ionosphere. Therefore, extra data from other sources such as ionosonde and/or inherent radar are desirable to provide more information on the top side and bottom-side ionosphere behavior during an eclipse. Further modeling studies are also required in order to reproduce the experimental results.

As far as the inconsistent relationship of regional maximum depression to the regional maximum solar obscuration is concerned, it is here suggested that other mechanisms must be considered. The geographical latitude of 25°, or geomagnetic latitude of 14°, located at one hump of the equatorial anomaly which is characterized by very high electron density. The hump phenomenon can be explained by the $\boldsymbol{E}\times\boldsymbol{B}$ electrodynamic drift and the diffusion of plasma along the geomagnetic field lines. Apparently the solar eclipse reduces the intensity of the equatorial fountain, but the mechanism inside needs to be solved.

Acknowledgments: The authors gratefully acknowledge the assistance of colleagues of the research group-Prof. M. Tian and Prof. S. Y. Ma - who participated in the experiment. Thanks are also due to the Ionospheric Research Group of Wuhan Institute of Physics and Institute of Space Science in National Central University, for providing the data.

References:

[1] Olatunji E O. An eclipse in the equatorial *F*-region [J]. *J Atmos Terr Phys*, 1967, **29**: 267-275.

[2] Fritz R B. Response of ionosphere and exosphere electron contents to a partial solar eclipse[J]. *J Geophys Res*, 1968, **73**: 4994-4998.

[3] Klobuchar J A. Ionospheric total electron content measurements in solar eclipse [J]. *Natl Sci Found*, 1973, **Bull5**: 80-84.

[4] LI Jun. Observation of the ionospheric total electron content during the solar eclipse of February 16, 1980 [J]. *Chinese J of Geophys*, 1981, **24**: 252-256(Ch).

[5] Yeh K C. Ionospheric response to a solar eclipse in the equatorial anomaly region[J]. *Terrestrial, Atomosphere and Oceanic Sciences*, 1997, **8**: 165-178.

[6] Xu J S. Observations of the ionospheric total electron contents during the solar eclipse of october 24, 1995 by Using the GPS Beacon [J]. *Terrestrial, Atomosphere and Oceanic Sciences*, 1997, **8**: 179-188.

[7] CHEN Pei-ren, The ionospheric response to the atmospheric quasi-biennial oscillation [J]. *Chinese J of Geophys*, 1992, **35**: 294-303(Ch).

[8] Sardon E A. Estimation of total electron content using GPS data: How stable are the differential satellite and receiver instrumental biases [J]. *Radio Sci*, 1997, **29**: 577-586.

[9] Evans J V. An *F*-region eclipse[J]. *J Geophys Res*, 1965, **70**: 131-142.